Research Square

Preprints are preliminary reports that have not undergone peer review.
They should not be considered conclusive, used to inform clinical practice,
or referenced by the media as validated information.

The FfMYB15-FfLAC9 Module Couples Mycelial Lignin Degradation to Fruiting Body Morphogenesis in Flammulina filiformis

Ningning Liu
Shanxi Agricultural University
Huixin Liu
Shanxi Agricultural University
Jingyao Wang
Shanxi Agricultural University
Hua Li
Shanxi Agricultural University
Zehua Zhang
Shanxi Agricultural University
Junlong Meng
Shanxi Agricultural University
Jingyu Liu
liujingyu80@126.com
Shanxi Agricultural University

Research Article

Keywords: Flammulina filiformis, Laccase, Lignin degradation, Fruiting body morphogenesis, Transcriptional regulation

Posted Date: September 8th, 2026

DOI: https://doi.org/10.21203/rs.3.rs-10783605/v1

License: This work is licensed under a Creative Commons Attribution 4.0 International License.
Read Full License

Additional Declarations: No competing interests reported.

The FfMYB15-*FfLAC9* Module Couples Mycelial Lignin Degradation to Fruiting Body Morphogenesis in *Flammulina filiformis*

Ningning Liu[a,b], Huixin Liu[a,b], Jingyao Wang[a,b], Hua Li[a,b], Zehua Zhang[a,b], Junlong Meng[a,b], Jingyu Liu[a,b*]

[1] College of Food Science and Engineering, Shanxi Agricultural University, Taigu 030801, Shanxi, China

[2] Key Laboratory of Shanxi Province for Loess Plateau Edible Fungi, Taigu 030801, Shanxi, China

[3] Shanxi Engineering Research Center of Edible Fungi, Taigu 030801, Shanxi, China

[*]Corresponding authors: liujingyu80@126.com; sxndcmc@163.com

ABSTRACT

The regulatory linkage between mycelial nutrient acquisition and fruiting body morphogenesis remains largely obscure in macro-fungal crops, despite its importance for commercial cultivation. Through genome-wide and expression profiling, we identified FfLAC9 as a key gene associated with the transitions from ligninolytic metabolism to fruiting body morphogenesis in *Flammulina filiformis*. Overexpression of *FfLAC9* enhanced extracellular laccase activity and lignin degradation in substrate, and promoted primordium initiation, additionally accelerated pileus differentiation and stipe elongation. Conversely, RNAi-*FfLAC9* not only exhibited opposite effects on these traits but also altered pileus pigmentation. Critically, we discovered that FfMYB15 as a direct transactivation activator of the *FfLAC9* promoter, as validated by Y1H, EMSA, and dual-luciferase assays. Collectively, these findings uncover the FfMYB15-*FfLAC9* module functions as a critical regulation switch linking mycelial lignin degradation and transformation capacity to fruiting body morphogenesis, offering a distinct genetic target for improving cultivation efficiency of *F. filiformis*, even related macro-fungi..

Keywords: *Flammulina filiformis*; Laccase; Lignin degradation; Fruiting body morphogenesis; Transcriptional regulation

1. Introduction

The coordination between extracellular lignocellulose degradation and the initiation of fruiting body development represents a critical yet mechanistically unresolved checkpoint in the life cycle of wood-decaying macrofungi.

Lignocellulose, the major component of agricultural wastes, serves as the core carbon source for edible fungi cultivation [1]. As saprophytes, edible fungi rely on extracellular lignocellulolytic enzymes to decompose lignocellulose into absorbable small-molecule nutrients, which regulates mycelial colonization, primordium differentiation, and fruiting body development [2]. This correlation has become a research focus in the optimization of the edible fungi industry and the valorization of agricultural waste [3]. The degradation process is synergistically regulated by multiple enzyme systems with distinct stage-specific characteristics, among which laccase is widely recognized as a key contributor [4].

Laccases, a class of multicopper oxidases, are pivotal in diverse physiological and ecological processes across plants, fungi, bacteria and insects [5, 6].Their capacity to oxidize a broad spectrum of phenolic substrates underpins significant applications in environmental bioremediation and industrial biotechnology [7]. Among these sources, fungal laccases are particularly notable for their high catalytic efficiency and crucial roles in fungal survival and adaptation [8], extending beyond classical lignin degradation to encompass stress responses, fruiting body formation, developmental regulation, melanin biosynthesis, and pathogenic virulence [9-11].

In macro-fungi, laccases have been reported to be closely linked to substrate utilization and mycelial vitality [12]. Key examples include *PoLac12* from *Pleurotus ostreatus* [13, 14],

lcc3 from *Auricularia heimuer* [15], *PeLac5* from *Pleurotus eryngii* [16], *Lcc9, Lac1* and *Lac5* from *Coprinopsis cinerea* [17, 18], *Lelcc1* from *Lentinula edodes* [19]. During fruiting body morphogenesis, specific laccases exhibit stage-specific expression and direct regulatory functions. In *P. ostreatus,* silencing of the *lacc2* gene significantly impairs fruiting body development [13]. Similarly, laccases such as *GL16401* and *GL19134* were markedly induced the transition from primordium to mature fruiting body, and coordinated the synthesis of bioactive compounds in *Ganoderma lucidum* [20]. In *Pycnoporus cinnabarinus*, laccase is integral to vivid red pigment synthesis and modulated by carbon sources, constituting the core molecular mechanism for pigment production [21]. Taken together, these findings highlight the central and multifaceted contributions of laccases to fungal morphogenesis and physiology. Nevertheless, the transcriptional mechanisms that coordinate laccase expression with nutrient metabolism across critical developmental transitions remain largely unknown.

F. filiformis has emerged as a promising model system for studying fungal genetics, developmental biology, biochemistry, and substrate utilization [22, 23]. In the cultivation of *F. filiformis*, yield and quality are primarily determined by the efficiency of substrate utilization and the precise manipulation of fruiting body development [24, 25]. Nevertheless, the precise mechanism by which lignin decomposition drives reproductive development has yet to be fully clarified. Laccases play a central role by influencing both mycelial metabolism and fruiting body formation [26]. MYB transcription factors are widely acknowledged as key regulators of fungal morphogenesis. In *F. filiformis*, our prior research demonstrated their significant involvement in this process. Specifically, FfMYB13 suppresses stipe browning and lignification by activating Ff-FeSOD1 and genes involved in cell wall biosynthesis [27].

FfMYB9 and FfMYB13 coordinately regulate primordium formation and stipe elongation by transcriptionally activating FfHyd19 [28]. Genome-wide analysis identified FfLAC9 as a developmentally regulated laccase gene harboring a putative MYB-binding motif in its promoter region.To date, the direct regulatory relationship between MYB transcription factors and laccase-mediated lignin degradation during fruiting body development in edible mushrooms remains largely unknown.

A genome-wide survey was conducted to systematically identify members of the laccase gene family in *Flammulina filiformis*. Functional genetic and molecular analyses demonstrated that *FfLAC9* is indispensable for efficient lignin degradation and normal fruiting body morphogenesis. Furthermore, we demonstrated that the MYB transcription factor *FfMYB15* directly binds to the *FfLAC9* promoter and transcriptionally activates its expression. Collectively, our findings uncover a previously unrecognized MYB–laccase regulatory module that coordinates lignocellulose utilization with fruiting body development, providing valuable molecular targets for genetic improvement and molecular breeding of edible mushrooms.

2 Materials and methods

2.1. Fungal Material and Preparation

The *F. filiformis* strain Ff813 was obtained from the Shanxi Edible Fungi Germplasm Resource Collection Center. Mycelia were pre-cultured was conducted on potato dextrose agar (PDA) supplemented with 200 μM ABTS for laccase activity screening, with incubation at 28°C for one week [29]. The mycelial plugs were then inoculated onto a solid substrate containing 78% cottonseed hulls, 20% bran, 1% dextrose, and 1% gypsum, and cultured in darkness at 25°C for 25 days. After complete substrate colonization, the cultures were

transferred to a fruiting chamber maintained at 10–12°C, 300–400 lx light intensity, and 80–90% relative humidity to induce primordia formation. Fruiting bodies were harvested 25–30 days after induction.

2.2. Gene cloning

Total RNA was extracted with the Quick RNA Isolation Kit (Omega, USA). cDNA was synthesized using HiScript® II Q RT SuperMix with gDNA Wiper (Vazyme, Nanjing, China). The *FfMYB15* sequence was obtained from in-house genomic data, and primers designed with Primer Premier 5.0 were synthesized commercially (Tsingke). Gene cloning was performed using I-5™ 2× High-Fidelity Master Mix (Tsingke), with primer sequences provided in Table S3.

2.3. Identification of LAC gene family

Since the three conserved LAC domains—copper oxidase (PF00394), copper oxidase_2 (PF07731), and copper oxidase_3 (PF07732)—are all essential for LAC proteins, their corresponding Hidden Markov Model (HMM) profiles were employed to query the *F. filiformis* (KACC42780) protein database using the HMMER program , with an E-value cutoff set at 1e-5. Candidate genes were further validated for the complete laccase domain using SMART and HMMSCAN In addition, the online software program NCBI-CDD was used to verify the functional domain of the identified Cu-oxidase candidate proteins. Chromosomal locations and gene structures of the *FfLAC* family were analyzed and visualized with TBtools. Protein physicochemical properties, including molecular weight, isoelectric point, aliphatic index, and instability index, were predicted using the ExPASy ProtParam tool. Subcellular localization was predicted with Cell-PLoc 2.0 . Homologous laccase sequences from *Arabidopsis thaliana*,

Saccharomyces cerevisiae, *Penicillium vulpinum*, and *Lentinula edodes* were obtained via BLAST against the UniProt database. A phylogenetic tree was constructed in MEGA11（Supplementary Table S1） using the neighbor-joining method (Poisson model, 1000 bootstrap replicates) and visualized with iTOL .

2.4. Sequence Analysis of FfLAC Genes

Exon and intron distribution patterns were predicted via GSDS2.0 For motif analysis, the MEME suite [30]was applied with the following settings: maximum motif number set to 15, motif width optimized between 10 and 50, and occurrence restricted to zero or one per sequence. Protein motifs and corresponding gene structures were subsequently visualized using TBtools under default parameters [31].

2.5. Expression patterns and analysis of the FfLACgene family in F. filiformis

Transcriptomic analysis across multiple developmental stages of *F. filiformis* strain Ff813 allowed for a comprehensive characterization of *FfLAC* gene expression profiles. Gene expression levels were calculated as log2(FPKM) values and visualized using TBtools [31]. To examine expression dynamics under different physiological conditions, samples from key developmental phases—mycelium, primordium, young fruiting body, and mature fruiting body—were collected for quantitative analysis. All qRT-PCR assays were conducted in technical triplicates, with β-actin (GenBank Accession No. AFM83888) employed as the internal reference gene [32]. The amplification protocol included initial denaturation at 95 °C for 3 s, followed by 40 cycles of denaturation at 95 °C for 3 s, annealing at 60 °C for 32 s, and extension at 72 °C for 3 s. Relative expression levels were determined using the $2^{-\Delta\Delta Ct}$ method [33], with target gene primer sequences listed in Supplementary Table S3.

2.6. Overexpression and RNAi Vector Construction

The *FfLAC9* overexpression vector was generated by performing *SpeI/PspOMI* double digestion [34]on the OE plasmid, followed by homologous recombination with the *FfLAC9* cDNA insert. For RNAi vector construction, the FfLAC9-sense fragment was first cloned into *SpeI/BglII*-digested RNAi plasmids, and then the *FfLAC9*-antisense fragment was inserted into *SpeI/PspOMI* linearized vectors. All recombinant constructs were subsequently transformed into Agrobacterium tumefaciens strain GV3101. Primer sequences used for vector assembly are listed in Table S3.

2.7.Generation of mutant strains

The experiment began with the inoculation of *F. filiformis* (strain Ff813) mycelia onto a PDA plate, followed by incubation at 28 °C for 5 days. A 5 mm diameter agar plug was then excised from the colony edge and transferred into CYM liquid medium for an additional 2 days of culture under the same temperature conditions. Simultaneously, recombinant *A. tumefaciens* strains carrying overexpression (OE) or RNA interference (RNAi) constructs were propagated. Bacterial cells from 50 mL culture were harvested by centrifugation at 5000 rpm and 4 °C for 15 min, and subsequently resuspended in IM medium for a 5 h induction period. The pre-cultured mycelial pellets were combined with the induced *A. tumefaciens* suspension and co-cultured on IM solid medium in darkness at 28 °C for 5 h. Following co-culture, the material was transferred to CYM medium supplemented with 8 μg/mL hygromycin and 50 μg/mL cefotaxime for selection. After 20–30 days of incubation, positive transformants were successfully obtained [34].

2.8. Determination of the mycelial biomass

Mycelial biomass was determined through liquid culture under sterile conditions. Twelve synchronously growing *F. filiformis* mycelial discs were inoculated into 100 mL of potato dextrose broth (PDB) in a 250 mL Erlenmeyer flask and incubated at 25 °C with shaking at 150 rpm. Each treatment included three biological replicates. After 12 days of cultivation, the mycelia were collected by filtering the medium through four layers of gauze, washed three times with sterile water, and dried to constant weight at 80 °C. The resulting dry weight was recorded as mycelial biomass. Take an appropriate amount of fermentation broth or mycelial culture, centrifuge at 4°C and 12,000 × g for 15 minutes, and collect the supernatant as the crude enzyme solution. Reserve for later use.

2.9. Determination of Enzyme Activity

The crude enzyme solution was obtained by centrifuging 2 mL of fermentation broth (collected as described in Section 2.8) at 12,000 r/min for 10 minutes at 4 °C. Laccase activity was determined in a reaction mixture containing 2.7 mL of 0.1 mol/L acetate buffer (pH 4.5), 0.2 mL of 0.5 mol/L ABTS, and 0.1 mL of the crude enzyme solution. After incubation at 25 °C for 3 minutes, the reaction was stopped on ice, and absorbance was measured at 420 nm using a microplate reader. One unit (U) of enzyme activity was defined as the amount of enzyme that oxidizes 1 μmol of ABTS per minute. Boiling-inactivated crude enzyme solution served as the control, with three replicates per sample.

2.10. Lignocellulosic Composition Analysis

Fresh cultivation substrates of F. velutipes were oven-dried at 60 °C to constant weight, ground, and passed through a 40-mesh sieve for subsequent analysis. Lignocellulosic components—namely hemicellulose, cellulose, and acid-insoluble lignin (ADL)—were

187 determined on a dry-weight basis using a modified Van Soest detergent fiber system.

188 Briefly, 1.000 g of dried substrate powder was refluxed for 1 h with 100 mL of neutral
189 detergent solution, 0.5 g of anhydrous sodium sulfite, and decalin as a defoaming agent. The
190 mixture was then vacuum-filtered through a pre-weighed G4 sand-core crucible. The retained
191 residue was rinsed successively with hot distilled water until neutral pH, washed with acetone
192 and ethanol, and dried at 105 °C to constant weight to determine neutral detergent fiber (NDF).
193 The NDF residue was subsequently refluxed for 1 h in 100 mL of acid detergent solution,
194 followed by identical filtration and drying procedures to obtain acid detergent fiber (ADF).

195 The ADF residue was subjected to hydrolysis with pre-cooled 72% (w/w) H_2SO_4 at 25 °C
196 for 4 h under continuous shaking. After dilution with distilled water and overnight static
197 incubation, the residual solids were filtered, washed free of acid, and dried at 105 °C. The dried
198 residues were then incinerated in a muffle furnace at 575 °C for 4 h until constant ash weight
199 was achieved.

200 Component contents were calculated on a dry substrate weight basis (w/w %) as follows:

201 Hemicellulose = NDF − ADF

202 Cellulose = ADF − acid-hydrolyzed residue mass fraction

203 ADL = (mass loss of acid-hydrolyzed residue after ashing / initial dry substrate mass) ×
204 100

205 Each treatment comprised three biological replicates and two technical duplicates, with all
206 gravimetric measurements performed to an accuracy of 0.1 mg. A certified corn stover standard
207 biomass was analyzed in each batch to verify method accuracy and ensure recovery consistency.

208 ***2.11. Color Measurement***

Surface color parameters of samples were determined with a CR-400 chroma meter (Konica Minolta Sensing Inc., Osaka, Japan) equipped with an 8 mm measuring aperture, following the CIE 1976 Lab* color space standard[35]. The instrument was set with D65 standard illuminant and a 10° standard observer angle before testing. A complete calibration procedure was strictly implemented prior to each batch of measurements: the equipment was powered on and preheated for 15 min to stabilize the internal light source; the measuring window was wiped clean with lint-free cloth, followed by sequential zero calibration with the matched standard black tile and full reflectance calibration using the factory-provided standard white calibration tile. At least five non-overlapping random positions on each sample surface were selected for independent detection, and the arithmetic average of valid readings was adopted as the final color parameter of each specimen.

The total CIE 1976 color difference ($\Delta E^*_{a\beta}$) between treatment groups and control groups was calculated using the standardized formula below:

$$\Delta E=\sqrt{(\Delta L^*)^2+(\Delta a^*)^2+(\Delta b^*)^2}$$

where ΔL^*, Δa^* and Δb^* referred to the differences in L*, a*, and b* values between paired comparative samples, respectively.

2.12. Detection of ROS in Mycelium Using DCFH-DA Fluorescent Probe

Intracellular ROS levels in *F. filiformis* mycelia were quantified using the fluorescent probe 2′,7′-dichlorodihydrofluorescein diacetate (DCFH-DA）[36, 37]. Mycelial samples were incubated with the DCFH-DA working solution under dark conditions at 28°C for 30 minutes, followed by washing with phosphate-buffered saline (PBS) to remove unbound probe. Fluorescence images were captured for all samples under identical microscopy settings using a

fluorescence microscope (e.g., Zeiss Axio Imager A1). The average fluorescence intensity of all mycelia in each field of view was quantified using image analysis software (e.g., ZEN software). The relative ROS level was expressed as the mean fluorescence intensity per unit area of mycelium.

2.13. Identification and Visualization of Cis-Regulatory Elements in FfLAC Gene Promoters

The promoter regions (2000 bp upstream of the translation initiation site) of the *FfLAC* genes were extracted from the *F. filiformis* genome. Cis-regulatory elements within these sequences were identified using PlantCARE [38]. The resulting data were visualized with TBtools, a bioinformatics platform for graphical representation of biological data [31].

2.14. Subcellular localization analysis

FfMYB15 was PCR-amplified and cloned into pBI121-EGFP (*XhoI/SalI*) via homologous recombination [39].The pBI121-EGFP-FfMYB15 construct and the empty vector were introduced into *A. tumefaciens* strain GV3101. Bacterial suspensions were prepared in an osmotic buffer containing 10 mM MES, 150 μM acetosyringone, and 10 mM $MgCl_2$ (pH 5.6), adjusted to an OD_{600} of 0.5, and then infiltrated into leaves of *N. benthamiana.* EGFP signals were visualized 60–72 h later by confocal microscopy (Leica).

2.15. Dual-luciferase assay (LUC)

A dual-luciferase reporter assay was conducted. The *FfLAC9* promoter (2 kb) was inserted into pGreenII0800-LUC (*FfLAC9 promoter*-LUC), and the stop codon removed *FfMYB15* CDS was cloned into pGreenII62-SK (CaMV35S-FfMYB15). Constructs were transformed into *Agrobacterium* GV3101 . Bacterial cultures ($OD_{600} \approx 1.0$) were mixed (effector:reporter = 9:1), incubated for 2 h, and co-infiltrated into *N. benthamiana* leaves. Controls included

CaMV35S-FfMYB15+LUC and CaMV35S + *FfLAC9 promoter*-LUC. After 24 h dark (25 °C) and 24 h light, leaves were treated with 1.5 mM luciferin (5 min dark) and imaged with a Tanon 5200 system (≥ 20 replicates) [40] .

2.16. Yeast One-Hybrid (Y1H)

FfMYB15 was cloned into pGADT7. The *FfLAC9* promoter was inserted into PHIS2-pro (EcoRI/SacI) to create a bait plasmid, which was transformed into yeast Y187. Transformants were selected on SD/-Trp and screened on SD/-Leu/-Trp with 3-AT to determine inhibitory concentration. The bait and pGADT7-FfMYB15 were then co-transformed into Y187. Co-transformants were selected on SD/-His/-Leu/-Trp with the predetermined 3-AT concentration, incubated for 2–5 days, and assessed for growth to determine regulatory interaction.[41].

2.17.Promoter Analysis and Electrophoretic Mobility Shift Assay (EMSA) of FfLAC9

Genomic DNA was extracted from *F. filiformis* using a commercial plant DNA extraction kit (Xinjing, China). A 2 kb region upstream of the *FfLAC9* coding sequence was amplified and sequenced with primers listed in Table S3. The coding sequence of *FfMYB15* was cloned into the pCold I plasmid (via *KpnI/PstI*) and heterologously expressed in *E. coli* BL21(DE3) [42].His-tagged FfMYB15 protein was induced with 0.5 mM IPTG at 16 °C for 12 h, followed by purification via Ni-NTA affinity chromatography (TransGen Biotech, China). Two 46 bp fragments spanning the predicted MYB-binding motifs in the *FfLAC9* promoter were synthesized and biotin-labeled using a commercial kit (Beyotime, China). For EMSA, the biotinylated probes were incubated with purified His-FfMYB15 in the presence or absence of unlabeled competitor DNA, and protein–DNA interactions were detected using a chemiluminescent EMSA kit (Beyotime, China).

2.18. Statistical analysis

All experiments were performed with at least three independent biological replicates and three technical replicates for each sample. Data were presented as mean ± standard error (SE). One-way analysis of variance (ANOVA) followed by Duncan's multiple range test was conducted via SPSS 26.0 software. Significance thresholds were set as $P < 0.05$ (significant) and $P < 0.01$ (extremely significant). Pearson correlation analysis with two-tailed significance test was used for gene expression correlation calculation. This statistical strategy is consistent with all figure legends.

3. Results

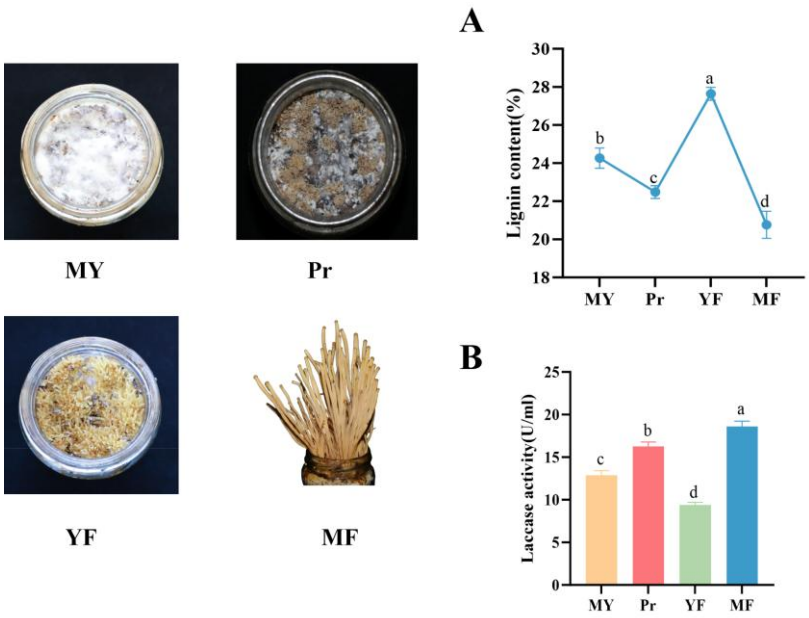


Figure 1. Dynamic changes of residual lignin content (A) and extracellular laccase activity (B) in cultivation substrate at four developmental stages of *F. filiformis*. MY, mycelium stage; Pr, primordium stage; YF, young fruiting body stage; MF, mature fruiting body stage. Different lowercase letters denote significant differences among treatments at $p < 0.05$. Data are expressed as mean ± standard deviation.

3.1 Dynamic lignin degradation and laccase activity of enoki mushroom substrate

The residual lignin content in cultivation substrate and extracellular laccase activity were determined at four key developmental stages of *F. filiformis*, including mycelium (MY), primordium (Pr), young fruiting body (YF) and mature fruiting body (MF) (Figure 1).

Substrate lignin content fluctuated significantly during mushroom development (Figure 1A). Lignin reached a moderate level of 24.27±0.53% at the MY stage, then decreased to the minimum value (22.48±0.34%) at the Pr stage due to extensive lignin biodegradation. Lignin accumulation peaked at 27.64±0.34% in the YF phase with suppressed lignin degradation, followed by a sharp decline to 20.76±0.71% at the MF stage. Significant differences in lignin content were observed among all stages ($p < 0.05$), as indicated by distinct lowercase letters.

Laccase activity exhibited an opposite dynamic pattern to residual lignin (Figure 1B). Basal laccase activity was 12.91±0.51 U/mL at MY, which significantly increased to 16.28±0.49 U/mL during primordium initiation (Pr). Laccase activity dropped to the lowest value (9.39±0.32 U/mL) at YF, consistent with maximal lignin residue at this stage. The maximum laccase activity of 18.60±0.61 U/mL was detected at MF, with significant intergroup differences across four stages ($p < 0.05$).

Overall, extracellular laccase activity was negatively correlated with substrate residual lignin, revealing that laccase-governed lignin degradation is precisely coordinated with morphological differentiation and fruiting body development of *F. filiformis.*

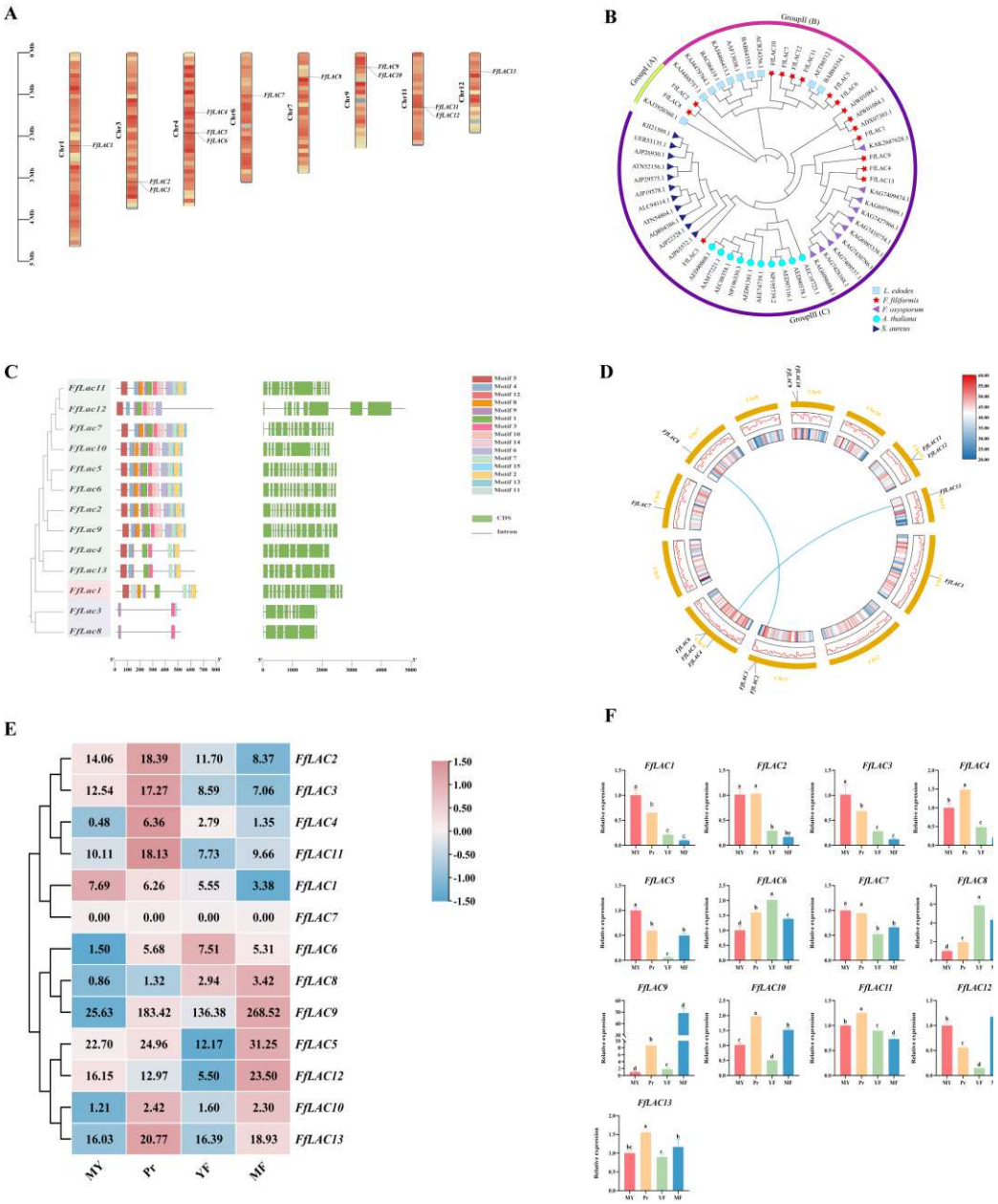


Fig. 2. Genomic Characterization of the *FfLAC* Gene Family. (A) Chromosomal distribution of *FfLAC* genes. (B)Phylogenetic analysis of laccase proteins. LACs from *F. filiformis* are highlighted with a red star, and related gene information is provided in Supplementary Table S2. (C) Structural and conserved motif patterns of *FfLAC* genes, with CDS shown as green boxes, introns as black lines, and twelve conserved motifs represented in distinct colors. (D) Combined visualization of chromosomal mapping, expression heatmap (log-transformed, scale: 20.00–60.00), and synteny relationships across Chr1–Chr12, offering insights into genomic organization and potential metabolic functions.(E) Expression clustering of laccase genes based on transcriptomic data. (F) qRT-PCR validation of differential laccase expression during developmental stages: mycelium (MY), primordium (Pr), young fruiting body (YF), and mature fruiting body (MF). Data (mean ± SE, *n* = 3) with different letters indicate significant differences ($P < 0.05$).

3.2. Phylogenetic relationships of the FfLAC gene family

A total of 13 putative laccase genes were identified in *F. filiformis* and designated *FfLAC1*

to *FfLAC13* according to their chromosomal distribution. The thirteen *FfLAC* family genes are unevenly distributed on chromosomes 1, 3, 4, 6, 7, 9, 11 and 12, with the highest number on Chr4 (5) and the lowest on Chr1 and Chr12 (1). To investigate the evolutionary relationships among members of the *FfLAC* gene family, we performed a phylogenetic analysis using the full-length protein sequences from *Lentinus edodes (L.edodes), Fusarium oxysporum (F.oxysporum), Arabidopsis thaliana (A.thaliana), Staphylococcus aureus (S. aureus),* and *Flammulina filiformis (F. filiformis)*. The results showed that members of the *FfLAC* gene family shared a closer phylogenetic relationship with those from *L. edodes*, *F. oxysporum*, and *S. aureus*, while exhibiting a more distant relationship with those from *A. thaliana*. This finding indicates that there are significant differences in the evolution of the *FfLAC* gene family between the aforementioned fungi and *A. thaliana*.

Bioinformatics analysis of family members revealed that the 13 *FfLAC* proteins consist of 509 (*FfLAC9*) to 762 (*FfLAC12*) amino acids, with relative molecular weights (MW) ranging from 54.63 kDa (*FfLAC9*) to 84.10 kDa (*FfLAC12*). The predicted isoelectric points (pI) span from 4.18 to 6.76, indicating that LAC genes function in an acidic subcellular environment. The instability index (II) values fall between 28.19 and 43.04. Most members of this family are hydrophilic and localized extracellularly. Additionally, all *FfLAC* proteins except *FfLAC7* and *FfLAC11* contain signal peptides, suggesting that this protein family performs similar functions and exerts its roles extracellularly.

3.3. Gene structures and conserved motifs of the FfLAC gene family

To gain deeper insights into the functional roles of the laccase (*LAC*) family in *F. filiformis*, we conducted a systematic analysis of their gene structures, conserved motifs, and

domains. NCBI-CDD analysis revealed that all *FfLAC* genes share conserved multicopper oxidase domains and exhibit similar structural patterns in terms of CDS and intron distribution. However, the number of introns varied across genes, with *FfLAC3* containing seven and *FfLAC5* possessing nineteen. An investigation of conserved motifs identified 15 distinct motifs (Motif 1~15). Among these, Motif 1 was found in 11 proteins, and Motif 2~5 were concurrently present in 10 members. Furthermore, a strong correlation was observed between motif conservation and phylogenetic relationship; *FfLAC2, FfLAC5, FfLAC6, FfLAC9*, and *FfLAC10*, which possess a similar set of motifs, were clustered closely on the phylogenetic tree. This consistency indicates that evolutionary relatedness underlies the conservation of gene structure and motifs, pointing to their putative functional relatedness.

3.4. Syntenic analysis of the FfLAC9 gene family members

Tandem and segmental duplications represent crucial mechanisms underlying the expansion of gene families. To investigate the expansion of the *FfLAC* gene family in *F. filiformis*, our analysis revealed that syntenic blocks between Chr3 and Chr7, as well as between Chr4 and Chr12, correspond to conserved ancestral genomic segments. These findings indicate the presence of extensive intraspecific synteny in the *F. filiformis* genome, providing a structural foundation for the functional conservation of genes.Further results demonstrate that the laccase gene family in *F. filiformis* is characterized by widespread intraspecific synteny, high sequence conservation, and a dispersed distribution across multiple chromosomes. This genomic architecture not only supports functional conservation among laccases but also facilitates functional divergence, enabling their involvement in diverse biological processes such as lignin degradation and pigment synthesis.

3.5. Tissue expression pattern of FfLACgene family

Analysis of FPKM-based expression patterns (Table S4) confirmed strong consistency between transcriptomic profiles and qRT-PCR results, validating the reliability of the transcriptomic dataset for subsequent molecular investigations. As illustrated in Figure 1E and F, most *FfLAC* genes were expressed across all developmental stages analyzed—mycelia, primordia, immature fruiting bodies, and mature fruiting bodies—though several genes displayed stage-specific expression patterns with notable quantitative differences. Among these, *FfLAC5, FfLAC9, FfLAC12,* and *FfLAC13* exhibited particularly high expression in specific developmental contexts. *FfLAC9* demonstrated consistently high transcript abundance throughout all stages, with significantly elevated expression in both primordia and mature fruiting bodies compared to other developmental phases. During the primordial formation stage of fruiting bodies, laccase gene expression increases sharply, accompanied by a peak in enzymatic activity. This upregulation precisely mediates hyphal knotting and cellular differentiation, establishing a critical foundation for subsequent morphogenesis. As the fruiting body matures, laccases translocate to the cortical cells and collaborate with hydrophobins. This synergistic interaction not only enhances the mechanical strength of the fruiting body surface, improving its resistance to environmental stressors such as physical damage and microbial invasion, but also contributes to pigment biosynthesis, thereby optimizing environmental adaptability.These findings indicate potential functional diversification among *LAC* gene family members in *F. filiformis* and suggest that *FfLAC9* may play a regulatory role in primordium development and fruiting body maturation.

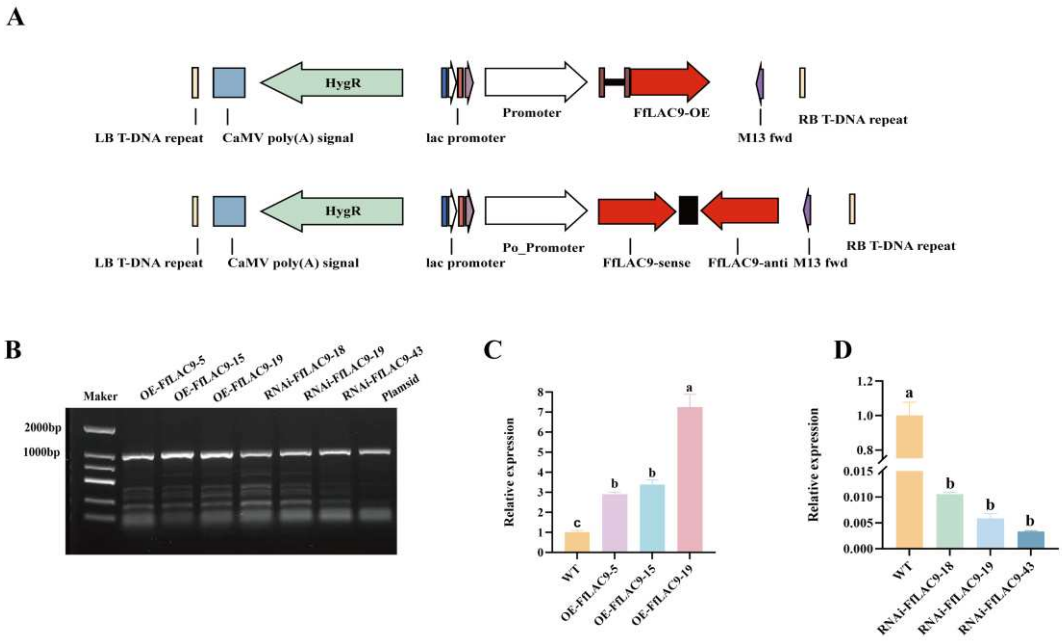


Fig. 3. Molecular and phenotypic characterization of *FfLAC9* transgenic strains in *F. filiformis* (A) Schematic of OE and RNAi vector construction. (B) PCR Verification of Hygromycin Resistance Gene (*hyg*) in Independent Transformants (C) *FfLAC9* expression levels assessed by qPCR; (E) Colony morphology on ABTS-containing medium (200 μM). (F) ROS accumulation visualized by SF7-AM staining (scale bar = 50 μm). (G) Mycelial biomass measured in fermentation cultures of WT, OE-FfLAC9-5, -15, -19 , and RNAi-FfLAC9-18, -19, -43 strains. (H)Enzyme activity assays of laccase in the WT and *FfLAC9* mutant strains. (I) Mycelial growth rate of different strains in cultivation bottles. Statistical significance between groups is indicated by different letters ($p < 0.05$, Duncan's test).

3.6. Acquisition of FfLAC9 mutant strain

To investigate the role of *FfLAC9* in *F. filiformis*, overexpression (OE) and RNA interference (RNAi) transformants were generated through Agrobacterium-mediated transformation (Fig. 3A). Successful plasmid integration was confirmed by PCR detection of the hygromycin resistance gene, which produced a ~1000 bp amplicon in the transgenic strains (Fig. 3B). Quantitative expression analysis revealed that *FfLAC9* relative expression levels in OE strains (OE-FfLAC9-5, -15, -19) were elevated by 2.9-, 3.4- and 7.2-fold compared to the wild type. In contrast, RNAi strains (RNAi-FfLAC9-18, -19, -43) showed near-complete gene silencing, with expression reduced by 99.2%, 99.6% and 99.7%, respectively (Fig. 3C, 3D).

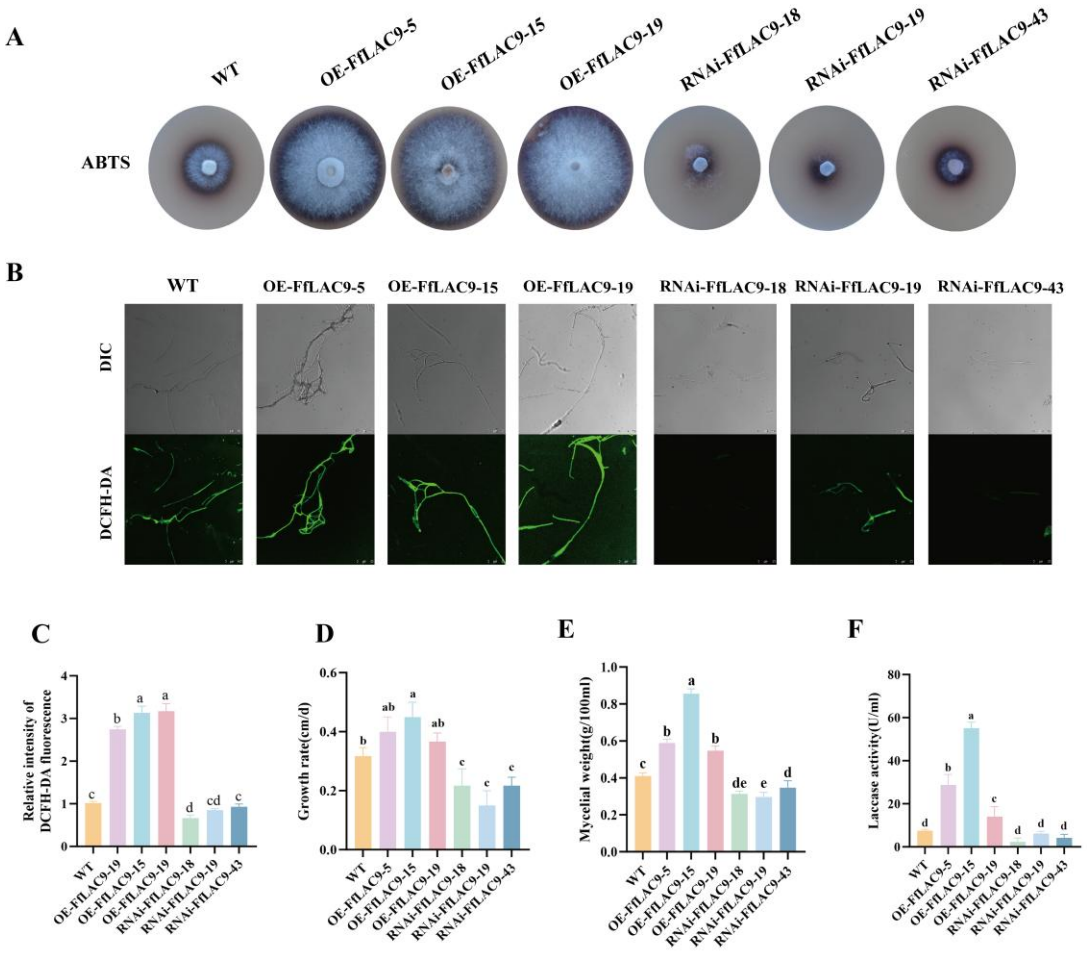


Fig. 4.(A) Colony morphology on ABTS-containing medium (200 μM). (B,C) DCFH-DA staining was performed to quantify the variation of ROS content in the mycelia of wild-type, FfLAC9 RNAi and FfLAC9 overexpression strains. (scale bar = 50 μm). (D) Mycelial biomass measured in fermentation cultures of WT, OE-FfLAC9-5, -15, -19 , and RNAi-FfLAC9-18, -19, -43 strains. (E)Enzyme activity assays of laccase in the WT and *FfLAC9* mutant strains. (F) Mycelial growth rate of different strains in cultivation bottles.Statistical significance between groups is indicated by different letters ($p < 0.05$, Duncan's test).

3.7. FfLAC9 positively regulates Laccase Activity and mycelial growth

The function of *FfLAC9* in laccase activity was evaluated using an ABTS-based plate assay. Genetic modulation of *FfLAC9* expression markedly influenced extracellular laccase activity, as indicated by distinct halo formation around mycelia cultured on medium containing 200 μM ABTS [29]. Consistent with a gain-of-function effect, the *FfLAC9*-overexpressing strain (OE-FfLAC9-5, -15, -19) generated a significantly larger and more intensely colored black halo relative to the wild-type (WT) strain. In contrast, RNAi-mediated silencing of *FfLAC9* led to a fainter and smaller halo, reflecting a loss-of-function phenotype. These visual outcomes

provide direct evidence that *FfLAC9* plays a critical role in the extracellular laccase system of this fungus. Morphological analysis further revealed that the OE-FfLAC9-5, -15, -19 strain developed a greater density of aerial hyphae with slenderer morphology at the mycelial edge, whereas the RNAi-FfLAC9-18, -19, -43 strain exhibited reduced aerial hyphae and shorter hyphal length (Fig. 4A).

Intracellular reactive oxygen species (ROS) in *F. filiformis* were quantified using DCFH-DA fluorescent probe staining, a reliable method for assessing oxidative stress in fungal hyphae. As demonstrated in Figure 4B.4C, the OE-FfLAC9-5, -15, -19 strain accumulated significantly higher ROS levels compared to both the wild-type and RNAi-FfLAC9-18, -19, -43 strains. Consistent with these findings, microscopic examination revealed distinct morphological differences among the strains: RNAi-FfLAC9-18, -19, -43 hyphae appeared thinner and shorter than wild-type hyphae, whereas OE-FfLAC9-5, -15, -19 strain developed notably longer and thicker hyphae.During the stages of fungal hyphal differentiation and fruiting body formation, reactive oxygen species (ROS) act as signaling molecules at appropriate concentrations to regulate cell differentiation. In contrast, laccases ensure the orderly progression of growth and development through two primary mechanisms: modulating intracellular ROS homeostasis and participating in cell wall modification and remodeling.

Further verification was obtained through ABTS-based assays measuring laccase activity in liquid culture supernatants and corresponding mycelial biomass. As shown in Figure 4D.4E, the OE-FfLAC9-5, -15, -19 strains exhibited approximately 3.8-, 7.3-, and 1.9-fold increases in laccase activity compared to wild-type (WT), whereas the RNAi-FfLAC9-18, -19, -43 strains showed reductions of 68.3%, 17.7%, and 45.0%, respectively. Parallel biomass measurements

382 revealed increases of 30.5%, 52.3%, and 25.4% for OE-FfLAC9-5, -15, -19 strains, while
383 RNAi-FfLAC9-18, -19, -43 strains displayed decreases of 24.4%, 26.8%, and 14.6%.
384 Evaluation of *FfLAC9*'s effect on substrate lignin degradation was conducted through
385 cultivation of wild-type, overexpression, and RNAi strains on cottonseed hull and wheat bran
386 substrates at 25 °C. Mycelial growth measurement showed significantly higher rates in OE-
387 FfLAC9-5, -15, -19 strains (0.317 ± 0.03, 0.400 ± 0.05, and 0.450 ± 0.05 cm/d) than in RNAi-
388 FfLAC9-18, -19, -43 strains (0.22 ± 0.06, 0.15 ± 0.05, and 0.22 ± 0.03 cm/d) (Fig. 4F).Full
389 substrate colonization was achieved by OE-FfLAC9-5, -15, -19 in 12 days, versus 15 days for
390 the wild type and 20 days for RNAi-FfLAC9-18, -19, -43. These findings demonstrate that
391 *FfLAC*9 enhances laccase activity and mycelial growth in *F. filiformis*, leading to accelerated
392 lignin degradation and a shortened growth period (Fig. 5A).
393 Substrate residual cellulose, hemicellulose and lignin were quantified to assess
394 lignocellulose degradation by WT, OE-FfLAC9-5, -15, -19 and RNAi-FfLAC9-18, -19, -43 in
395 *F. filiformis.* Post-cultivation, *FfLAC9* overexpression substrates contained far less residual
396 cellulose (averages: 22.50%, 20.59%, 18.81%) than WT (28.23%), while RNAi substrates
397 retained much higher cellulose (31.09%–33.29%). Hemicellulose followed the same pattern:
398 overexpression lines averaged 21.71%–23.65% hemicellulose versus WT's 25.95%, and
399 silenced strains held elevated hemicellulose residues (27.06%–28.28%). For lignin,
400 overexpression transformants exhibited stronger degradative capacity overall; WT lignin
401 averaged 25.58%, OE-FfLAC9-5, -15, -19 lines ranged 25.46%–25.90%, and RNAi-FfLAC9-
402 18, -19, -43 strains accumulated more residual lignin (24.64%–28.58%). These compositional
403 results confirm *FfLAC9* overexpression drastically enhances lignocellulose catabolism,

whereas *FfLAC9* knockdown suppresses cellulose and hemicellulose breakdown. This pattern aligns with higher ROS levels and extracellular laccase activity measured in *FfLAC9*-overexpressing mycelia（Figures 5B,5C,5D）.

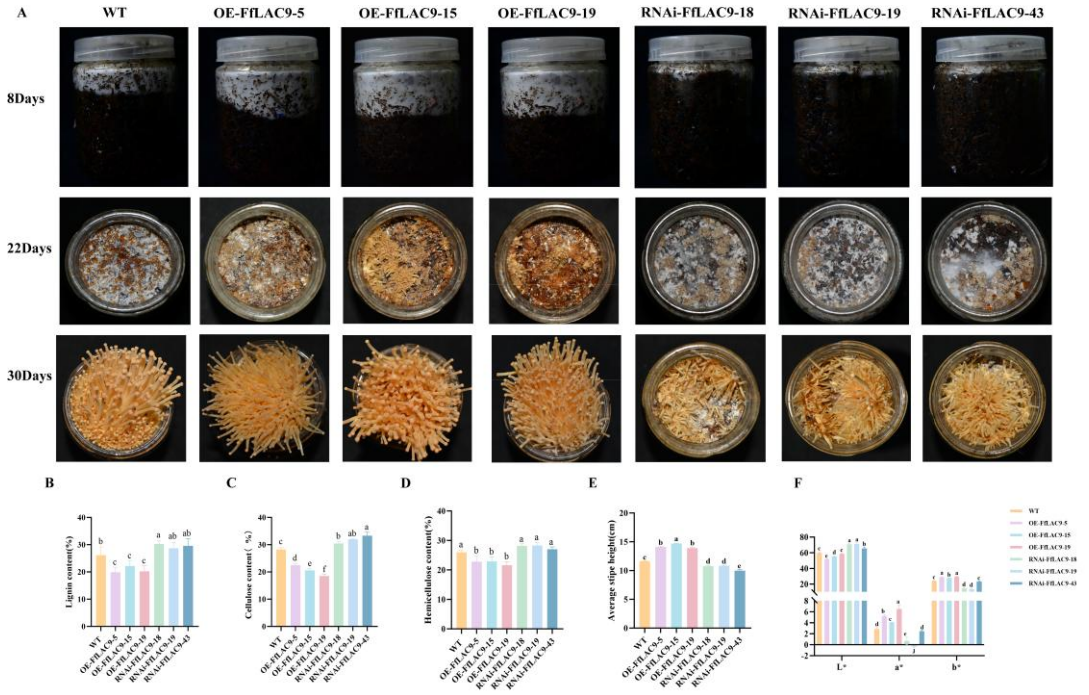


Fig. 5. *FfLAC9* positively regulates the degradation of lignin in the substrate and the development of fruiting bodies in *F. filiformis.* (A) Morphological comparison between the wild-type (WT) and the *FfLAC9* mutant strains during development from hyphal knot formation to mature fruiting bodies. (B-D) Contents of lignin, cellulose and hemicellulose in substrates of WT and *FfLAC9* mutant strains. (E) Average stipe height of fruiting bodies. (F) Color phenotypes of the WT and *FfLAC9* mutant strains. Different letters indicate statistically significant differences between samples ($p < 0.05$, Duncan's test).

3.8. FfLAC9 positively regulates primordia formation and fruiting body pigmentation of F. filiformis

Following 16 days of cultivation on cottonseed hull and wheat bran substrates, surface mycelia were mechanically removed and subjected to low-temperature induction for primordium formation. In wild-type strains, primordia appeared six days post-induction (22 days after inoculation). The OE-FfLAC9-5, -15, -19 strain demonstrated accelerated development, forming primordia two days earlier than the wild-type, with significantly increased primordia numbers and more intense yellow pigmentation. By day 30 post-

inoculation, the OE-FfLAC9-5, -15, -19 strain exhibited higher and thicker fruiting bodies with more uniform stipe heights, along with significantly greater fruiting body production compared to the wild-type. In contrast, the RNAi-FfLAC9-18, -19, -43 strain showed severely impaired development, with only sparse primordia formation or complete absence of primordia by day 22, accompanied by noticeably reduced pigmentation. By day 30, the RNAi-FfLAC9-18, -19, -43 strain produced only limited fruiting bodies with shorter and irregular stipe heights. Quantitative analysis revealed average stipe heights of 11.60 ± 0.11 cm for wild-type, compared to 14.13 ± 0.11 cm, 14.67 ± 0.08 cm, and 13.88 ± 0.19 cm for OE-FfLAC9-5, -15, -19 strains. The RNAi-FfLAC9-18, -19, -43 strains exhibited significantly reduced heights of 10.75 ± 0.13 cm, 10.81 ± 0.10 cm, and 9.98 ± 0.19 cm.

Color parameters (L*, a*, b*) of OE-FfLAC9-5, -15, -19 and RNAi-FfLAC9-18, -19, -43 strains were measured using the CIE L*a*b* system. The total color difference (ΔE) between strains reached 24.30, 22.04, and 10.24, indicating visually distinct phenotypes （Supplementary Figure 4）. This shift was characterized by a notable decrease in L* (from 69.25 to 55.17) and an increase in b* (from 17.10 to 28.71) in OE-FfLAC9-5, -15, -19, corresponding to darker and more yellow coloration, while a* remained stable. These changes suggest a role for *FfLAC9* in pigment synthesis and deposition in *F. filiformis*.

Together, these findings demonstrate that *FfLAC9* promotes primordium formation, pigment synthesis, and fruiting body development in *F. filiformis*.

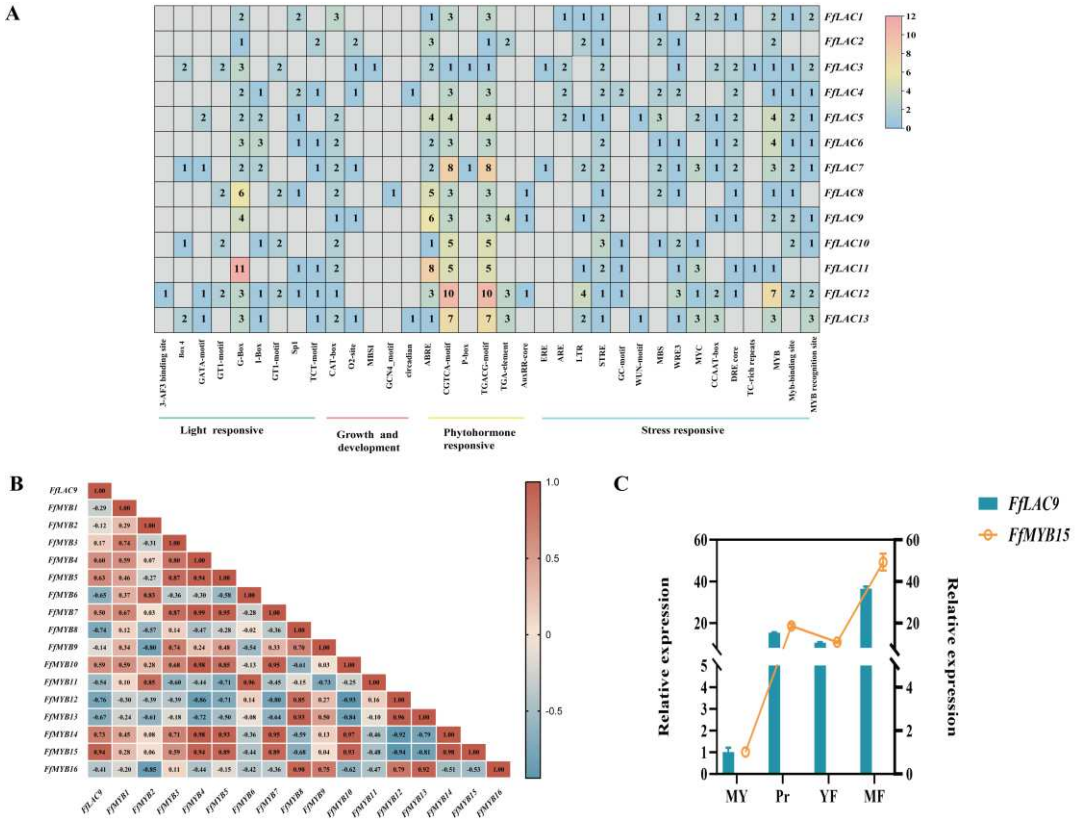


Fig. 6 .Proposed Interaction Between FfMYB15 and the *FfLAC9* Promoter (A) Analysis of cis-regulatory elements in the promoter regions of the *FfLAC* gene family. (B) Heatmap of correlation coefficients between the transcriptional levels of the *FfLAC9* and *FfMYB* family genes, derived from FPKM values in the transcriptome analysis. (C) Expression patterns of *FfLAC9* and *FfMYB15* across various developmental stages. Different letters denote statistically significant differences among samples (Duncan's test, $p < 0.05$).

3.9 FfMYB15 potentially regulate the expression of FfLAC9

The cis-acting elements within the *FfLAC* promoters were analyzed and categorized into four groups: light-responsive, growth and development-related, phytohormone-responsive, and stress-responsive elements.(Fig. 6A). All *FfLAC* promoters contained light responsive G-box element ,hormone-dependent growth, development, and defense process-regulating TGACG-motif element, high-temperature responsive STRE elements. MYB binding sites were also detected in the promoters of *FfLAC1*, *FfLAC3–FfLAC10*, and *FfLAC12*, indicating possible transcriptional regulation by MYB factors. As illustrated in Figure 6B, a significant positive correlation ($P < 0.05$) was observed between FfMYB15 and FfLAC9, with a Pearson

correlation coefficient of 0.94 across different developmental stages. We employed qRT-PCR to analyze the transcript levels of *FfMYB15* and *FfLAC9* at different developmental stages of *F. filiformis*, encompassing mycelium (MY), primordium (Pr), young fruiting body (YF), and mature fruiting body (MF).The transcriptional level trends of the two genes were consistent(Fig. 6C). The transcription levels from primordia to spores were higher than those at mycelian stage.Combined with the promoter analysis results of *FfLAC9*, MYB binding sites were identified. These results further indicate that the transcription factor FfMYB15 may have an association with *FfLAC9*.

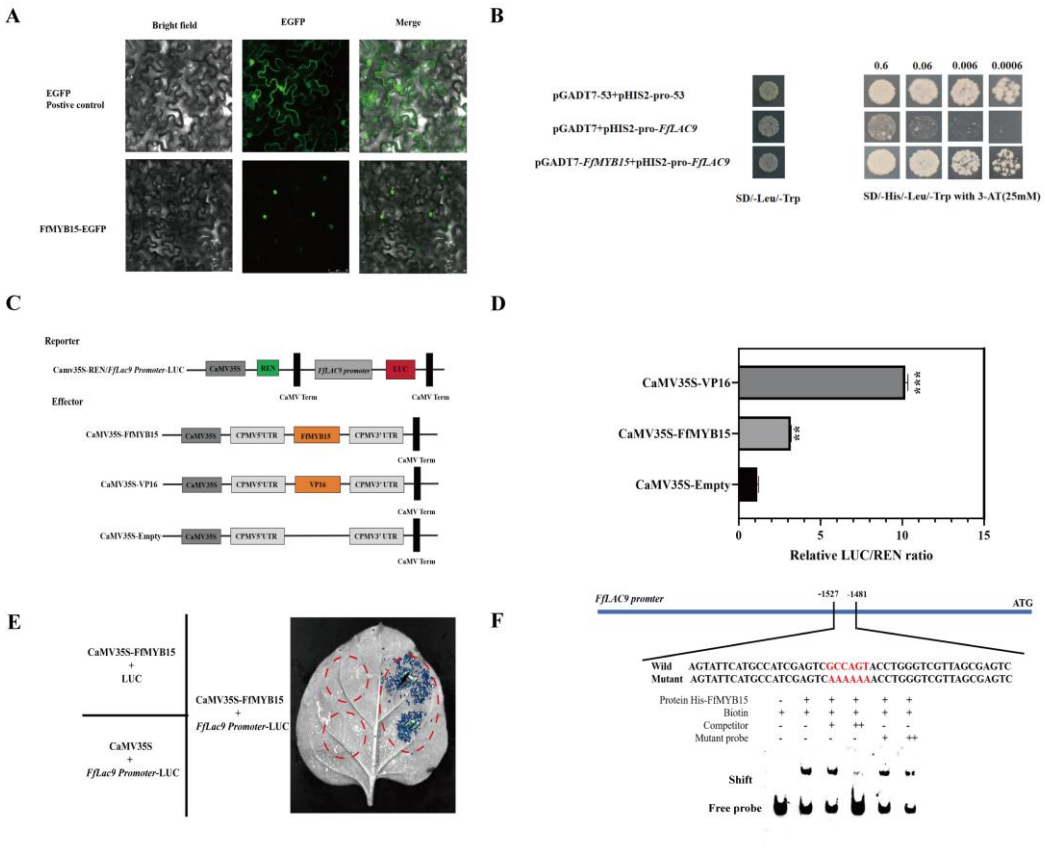


Fig. 7. Subcellular localization and transcriptional activity analysis of FfMYB15. (A) Subcellular localization. EGFP (positive control) and FfMYB15-EGFP fusion proteins were expressed in tobacco leaf epidermal cells and visualized by fluorescence microscopy at 60 h post-infiltration. Scale bar = 25 μm. (B) Y1H validation results. (C) Schematic of effector and reporter constructs used in dual-luciferase assays. (D) Transcriptional activation of *FfLAC9* by FfMYB15. The empty plasmid plus promoter group (Luc/Ren ratio = 1) served as the reference. Data are mean ± S.E.M. (n = 6); $^{**}P < 0.01$. (E) LUC imaging results for the binding and

activation abilities of FfMYB15 on the *FfLAC9* promoter, respectively. (F) Electrophoretic mobility shift assay (EMSA). Purified His-FfMYB15 was incubated with a biotin-labeled probe containing the MYB-binding cis-element from the *FfLAC9* promoter. Controls included reactions without protein ("-" protein) or without probe ("-" probe). Competition assays used increasing concentrations (+, ++) of unlabeled wild-type or mutant probes to confirm binding specificity.

3.10. The binding and activation effects of FfMYB15 on FfLAC9 promoter

Bioinformatic analysis revealed the presence of MYB transcription factor binding sites in the promoter region of *FfLAC9*, suggesting potential transcriptional regulation by MYB transcription factors. Since transcription factors require nuclear localization to function, subcellular localization of FfMYB15 was investigated through transient expression in tobacco leaves. The results showed exclusive nuclear localization of the FfMYB15-EGFP fusion protein, in contrast to the diffuse cytoplasmic and perinuclear distribution of EGFP alone(Fig. 7A).

A yeast one-hybrid assay (Y187-PHIS2-pro system) was employed to analyze transcription factor-promoter interactions. On SD/-Leu/-Trp medium, Control Groups (pGADT7-53 + pHIS2-pro-53) and (pGADT7 + pHIS2-pro-FfLAC9), and experimental group (pGADT7-FfMYB15 + PHIS2-pro-FfLAC9) showed similar growth. However, on selective medium containing 250 mM 3-amino-1,2,4-triazole (3-AT), both the positive control and experimental group demonstrated robust growth, while the negative control showed negligible growth, confirming the absence of self-activation and specific binding of FfMYB15 to the *FfLAC9* promoter (Fig. 7B).

Further validation through dual-luciferase assays (Fig. 7C) showed that CaMV35S-FfMYB15 significantly increased the LUC/REN ratio compared to CaMV35S-Empty when co-expressed with the *FfLAC9* promoter-driven reporter. Consistent with this, CaMV35S-FfMYB15 markedly enhanced *FfLAC9 promoter*-LUC-derived fluorescence in tobacco leaves

(Figs. 6D, 6E). These results demonstrate that FfMYB15 directly binds to and activates the *FfLAC9* promoter, thereby promoting laccase gene expression.

EMSA results demonstrated that purified His-FfMYB15 protein could form specific protein-DNA complexes with biotin-labeled wild-type *FfLAC9* promoter probe, producing clear shifted bands. The addition of excess unlabeled wild-type competitive probe gradually attenuated shifted band intensity, while mutant probe with disrupted MYB binding motif failed to compete for protein binding and did not eliminate the shift signal. No specific retarded band was observed in the absence of recombinant FfMYB15 protein, confirming the specific physical interaction between FfMYB15 and the MYB cis-element within *FfLAC9* promoter (Fig. 7F).

4. Discussion

Laccases are versatile enzymes involved in various fungal processes such as lignin degradation, morphogenesis, and stress adaptation. In different fungal species, laccase gene families exhibit significant evolutionary diversity and functional divergence [5]. Laccase genes have been identified in many macrofungi, including *C. cinerea* [43], *Agaricus bisporus* [44] and *P. ostreatus* [14]. In this study, 13 laccase isoenzyme genes were identified in the *F. filiformis* genome, representing an increase from the previously reported 11 genes [26], and were classified into three groups. These findings further highlight the evolutionary diversification of the laccase gene family and support the hypothesis that ancestral laccase genes underwent functional divergence, giving rise to specialized paralogs adapted to distinct stages of fungal development. [45]. Bioinformatic and protein structural analyses of these 13 genes revealed that their encoded proteins share high structural and phylogenetic homology

with previously reported laccases from *L. edodes*. The phylogenetic relationships among fungal laccases do not strictly follow species evolution but are closely associated with function [8], suggesting that *F. Filiformis* laccases may be functionally similar to those of *L. edodes*. Transcriptomic analysis of different developmental stages of *F. Filiformis* showed that *FfLAC9* is consistently highly expressed across all stages, with a significant increase during the primordium and mature fruiting body phases. These expression patterns suggest functional specialization among members of the *FfLAC* gene family and implies that *FfLAC9* may play a regulatory role in primordium development and fruiting body maturation. Furthermore, prediction of cis-acting elements in the *FfLAC9* promoter identified motifs associated with light, stress, and drought responses, as well as MYB transcription factor binding sites. Collectively, these findings suggest that *FfLAC9* contributes not only to stress adaptation but also to multiple biological processes associated with fungal growth, differentiation, and fruiting body development. [46, 47].

Laccases play a crucial role in various fungal physiological activities [48]. Through functional analysis of *FfLAC9*, this study reveals its dual role in the metabolism and development of *F. Filiformis*. On the one hand, overexpression of *FfLAC9* enhances extracellular laccase activity, promotes mycelial growth advantage, and thereby accelerates the degradation of lignin in substrates. On the other hand, it also facilitates primordium formation and fruiting body development. These findings align with previous reports in *Hypsizygus marmoreus*, where overexpression of *Lcc1* promotes mycelial growth and fruiting body formation [49]. Notably, RNAi-mediated knockdown of *FfLAC9* resulted in reduced pigmentation, suggesting that *FfLAC9* may be involved in the oxidative polymerization of

phenolic compounds during fruiting body development. Related studies have shown that different laccase isozymes in fungi can directly or indirectly regulate fruiting body development. For example, in *G. tsugae*, deletion of *Lcc1* leads to pale gray instead of the normal reddish-brown coloration in fruiting bodies, as well as shorter stipes, indicating that this gene is directly involved in pigment deposition and stipe elongation [50]. In *P. ostreatus*, silencing of *lacc2* affects cystidium formation, thereby interfering with normal primordium and fruiting body development [13]. Moreover, silencing of *L. edodes lcc1* not only inhibits mycelial morphological development [51], but also affects cell wall structure formation [52]. Collectively, these studies demonstrate that laccases play a key role in morphogenesis and the maintenance of cell wall integrity across various fungal species. Combined with the findings of the present study, it can be inferred that *FfLAC9* likely participates in regulating mycelial development, primordium differentiation, and fruiting body formation in *F. Filiformis* by degrading lignocellulosic substrates.

MYB transcription factors have been extensively identified as key regulators governing fundamental biological processes such as growth, development, and stress responses [53]. For instance, in *Betula platyphylla*, BplMYB46 enhances stress tolerance by activating genes involved in antioxidant defense (SOD and POD) and osmoprotection (P5CS), in addition to promoting secondary cell wall deposition [54]. In potato, StMYB168 functions collaboratively with StWRKY20 to modulate lignin biosynthesis. Moreover, together with StMYB24/144, it contributes to suberin metabolism during closing layer development [55]. However, transcriptional regulation in edible fungi, which represent major commercial fungal crops, has not received attention comparable to that given to traditional crops. Our recent

findings indicate that the FfMYB13 protein contributes to cell wall remodeling by modulating the expression of genes involved in cell wall synthesis. [27]. However, the precise molecular mechanisms underlying MYB-mediated regulation of laccase gene expression have yet to be fully characterized. In this study, yeast one-hybrid assays, electrophoretic mobility shift assays (EMSA), and dual-luciferase reporter assays collectively demonstrated that the FfMYB15 protein can bind to and directly activate the promoter of the *FfLAC9* gene, leading to its upregulated expression.

5. Conclusions

This study identified 13 laccase genes (*FfLACs*) in *F. filiformis* through genome-wide analysis. Functional characterization revealed that *FfLAC9* plays a central role in regulating fungal growth and development, as its overexpression significantly enhanced lignin degradation, mycelial growth, primordium formation, fruiting body pigmentation, and shortened the cultivation cycle. Furthermore, we demonstrated that the transcription factor FfMYB15 directly activates *FfLAC9* expression by binding to its promoter. Collectively, our findings establish a MYB-laccase regulatory axis that coordinates biomass nutrient utilization and developmental processes in *F. filiformis*, shedding novel light on the molecular mechanisms governing fungal physiology related to lignocellulose conversion and providing potential genetic targets for improving key industrial traits of edible mushrooms.

6. Declarations

6.1 Ethical Approval

Not applicable. This study only involved the cultivation and molecular biological analysis of *F. filiformis*, a common edible fungus, and did not involve any human participants, human

tissues, animal experiments, or field studies related to protected species. Therefore, ethical approval and informed consent are not required for this research.

6.2 Funding

This study was funded by the National Science Foundation of China (No. 32072647), the earmarked fund for Shanxi-Talent-Support-Program Technology-Innovation-Leading Talent-Project (No. SJYC2025035) and Shanxi Modern Agro-industry Technology Research System (No. 2026CYJSTX09-02).

6.3 Availability of data and materials

All data generated or analyzed during this study are included in this published article and its supplementary information files. The raw sequencing data, gene sequence information, and experimental datasets that support the findings of this study are available from the corresponding author upon reasonable request. All relevant materials used in this study are commercially available or preserved in the laboratory for public academic research use.

6.4 CRediT authorship contribution statement

Jingyu Liu: conceptualization and writing–review. Ningning Liu: conceptualization and methodology, and writing–original draft. Huixin Liu: software analysis, formal analysis, and visualization. Jingyao Wang and Hua Li: date curation. Zehua Zhang Formal analysis. Junlong Meng: resources and data curation.

6.5 Declaration of competing interest

All the authors declare that they have no competing financial interests or personal relationships that could have appeared to influence the work reported in this article

References

[1] F. Wang, L. Xu, L. Zhao, Z. Ding, H. Ma, N. Terry, Fungal Laccase Production from Lignocellulosic Agricultural Wastes by Solid-State Fermentation: A Review, Microorganisms 7(12) (2019) 665.

[2] A. Shankar, K.K. Jain, R.C. Kuhad, K.K. Sharma, Comparison of lignocellulosic enzymes and CAZymes between ascomycetes (*Trichoderma*) and basidiomycetes (*Ganoderma*) species: a proteomic approach, Z Naturforsch C J Biosci 80(1-2) (2025) 21–32.

[3] T. Yuliana, A. Fauziah, E. Mardawati, H. Marta, R. Safitri, A. Krama, Laccase Characterization from *Ganoderma lucidum* Grown in Pineapple and Coffee Waste Substrates under Solid Fermentation, Pak J Biol Sci 28(1) (2025) 16–26.

[4] A. Hatakka, Lignin-modifying enzymes from selected white-rot fungi: production and role from in lignin degradation, FEMS Microbiology Reviews 13(2-3) (1994) 125–135.

[5] G. Janusz, K.H. Kucharzyk, A. Pawlik, M. Staszczak, A.J. Paszczynski, Fungal laccase, manganese peroxidase and lignin peroxidase: gene expression and regulation, Enzyme Microb Technol 52(1) (2013) 1–12.

[6] I.L. Wu, K. Narayan, J.P. Castaing, F. Tian, S. Subramaniam, K.S. Ramamurthi, A versatile nano display platform from bacterial spore coat proteins, Nat Commun 6 (2015) 6777.

[7] S. Ridtibud, N. Suwannasai, A. Sawasdee, V. Champreda, C. Phosri, S. Sarp, N. Pisutpaisal, S. Boonyawanich, Screening of White-Rot Fungi Isolates for Decolorization of Pulp and Paper Mill Effluent and Assessment of Biodegradation and Biosorption Processes, Curr Microbiol 80(11) (2023) 350.

[8] P.J. Hoegger, S. Kilaru, T.Y. James, J.R. Thacker, U. Kües, Phylogenetic comparison and classification of laccase and related multicopper oxidase protein sequences, Febs j 273(10) (2006) 2308–26.

[9] A. Sapmak, K.J. Boyce, A. Andrianopoulos, N. Vanittanakom, The *pbrB* gene encodes a laccase required for DHN-melanin synthesis in conidia of T*alaromyces (Penicillium) marneffei*, PLoS One 10(4) (2015) e0122728.

[10] A. Cesur, R. Yamamoto, Y. Asada, A. Watanabe, Relationship between fruiting body development and extracellular laccase production in the edible mushroom *Flammulina velutipes*, Biochemistry and biophysics reports 29 (2022) 101204.

[11] S. Chen, W. Ge, J.A. Buswell, Molecular cloning of a new laccase from the edible straw mushroom *Volvariella volvacea*: possible involvement in fruit body development, FEMS microbiology letters 230(2) (2004) 171–176.

[12] S. Zhou, J. Zhang, F. Ma, C. Tang, Q. Tang, X. Zhang, Investigation of lignocellulolytic enzymes during different growth phases of *Ganoderma lucidum* strain G0119 using genomic, transcriptomic and secretomic analyses, PLoS One 13(5) (2018) e0198404.

[13] A. Armas-Tizapantzi, J.L. Martínez y Pérez, F.J. Fernández, G. Mata, L.V. Hernández-Cuevas, E. Ortiz Ortiz, E. García Nieto, A. Tomasini, E. Sierra-Palacios, J. Marcial-Quino, A.M. Montiel-González, Silencing of the Laccase (*lacc2*) Gene from *Pleurotus ostreatus* Causes Important Effects on the Formation of Toxocyst-like Structures and Fruiting Body, International Journal of Molecular Sciences 24(9) (2023) 8143.

[14] X. Jiao, G. Li, Y. Wang, F. Nie, X. Cheng, M. Abdullah, Y. Lin, Y. Cai, Systematic Analysis of the *Pleurotus ostreatus* Laccase Gene (*PoLac*) Family and Functional Characterization of *PoLac2* Involved in the Degradation of Cotton-Straw Lignin, Molecules 23(4) (2018) 880.

[15] X. Fan, Y. Zhou, Y. Xiao, Z. Xu, Y. Bian, Cloning, expression and phylogenetic analysis of a divergent laccase multigene family in *Auricularia auricula-judae*, Microbiological research 169(5-6) (2014) 453–462.

[16] Z. Li, Y. Zhou, C. Xu, J. Pan, H. Li, Y. Zhou, Y. Zou, Genome-wide analysis of the *Pleurotus eryngii* laccase gene (*PeLac*) family and functional identification of *PeLac5*, AMB Express 13(1) (2023) 104.

[17] J. Hu, Y. Zhang, Y. Xu, Q. Sun, J. Liu, W. Fang, Y. Xiao, U. Kües, Z. Fang, Gongronella sp. w5 elevates *Coprinopsis cinerea* laccase production by carbon source syntrophism and secondary metabolite induction, Applied microbiology and biotechnology 103(1) (2019) 411–425.

[18] M. Rühl, A. Majcherczyk, U. Kües, Lcc1 and Lcc5 are the main laccases secreted in liquid cultures of *Coprinopsis cinerea* strains, Antonie van Leeuwenhoek 103(5) (2013) 1029–1039.

[19] L. Yan, R. Xu, Y. Bian, H. Li, Y. Zhou, Expression profile of laccase gene family in white-rot basidiomycete *Lentinula edodes* under different environmental stresses, Genes 10(12) (2019) 1045.

[20] X. Xu, C. Li, F. Wu, S. Zhao, T. Chen, H. You, Y. Lin, X. Zou, Integrated transcriptomic and targeted metabolomic analysis reveals the key genes involved in triterpenoid biosynthesis of *Ganoderma lucidum*, Journal of Fungi 11(1) (2025) 57.

[21] U. Temp, C. Eggert, Novel interaction between laccase and cellobiose dehydrogenase during pigment synthesis in the white rot fungus *Pycnoporus cinnabarinus*, Applied and environmental microbiology 65(2) (1999) 389–395.

[22] X.-B. Liu, E.-H. Xia, M. Li, Y.-Y. Cui, P.-M. Wang, J.-X. Zhang, B.-G. Xie, J.-P. Xu, J.-J. Yan, J. Li, Transcriptome data reveal conserved patterns of fruiting body development and response to heat stress in the mushroom-forming fungus *Flammulina filiformis*, PLoS One 15(10) (2020) e0239890.

[23] Y.J. Park, J.H. Baek, S. Lee, C. Kim, H. Rhee, H. Kim, J.S. Seo, H.R. Park, D.E. Yoon, J.Y. Nam, H.I. Kim, J.G. Kim, H. Yoon, H.W. Kang, J.Y. Cho, E.S. Song, G.H. Sung, Y.B. Yoo, C.S. Lee, B.M. Lee, W.S. Kong, Whole genome and global gene expression analyses of the model mushroom *Flammulina velutipes* reveal a high capacity for lignocellulose degradation, PLoS One 9(4) (2014) e93560.

[24] J.Y. Liu, M.C. Chang, J.L. Meng, C.P. Feng, H. Zhao, M.L. Zhang, Comparative Proteome Reveals Metabolic Changes during the Fruiting Process in *Flammulina velutipes*, J Agric Food Chem 65(24) (2017) 5091–5100.

[25] B. Deng, B. Zhang, L. Xi, M. Chang, J. Meng, C. Feng, J. Liu, J. Xu, The Tissue Browning and Concomitant Toughening of Yellow *Flammulina filiformis* Stipes Is Caused by Oxidative Damage-Mediated Metabolic Disorder and Cell Wall Glycan Remodeling, J Agric Food Chem 71(44) (2023) 16593–16603.

[26] W. Wang, F. Liu, Y. Jiang, G. Wu, L. Guo, R. Chen, B. Chen, Y. Lu, Y. Dai, B. Xie,

674 The multigene family of fungal laccases and their expression in the white rot
675 basidiomycete *Flammulina velutipes*, Gene 563(2) (2015) 142–9.
676 [27] B. Zhang, X. Wei, L. Xi, Y. Qiao, M. Chang, B. Deng, J. Liu, Genome-wide
677 identification of the MYB gene family and FfMYB13 regulation analysis in cell
678 wall synthesis underlying tissue toughening process of yellow *Flammulina*
679 *filiformis* stipes, Int J Biol Macromol 288 (2025) 138660.
680 [28] L. Xi, X. Wei, N. Liu, Y. He, Y. Qiao, L. Chang, B. Deng, M. Chang, J. Liu,
681 Transcription factors FfMYB9 and FfMYB13 jointly activate the expression of
682 hydrophobin gene *FfHyd19* to mediate fruiting body morphogemesis in
683 *Flammulina filiformis*, International Journal of Biological Macromolecules
684 (2025) 145611.
685 [29] R. Bourbonnais, M.G. Paice, Oxidation of non-phenolic substrates: an expanded
686 role for laccase in lignin biodegradation, FEBS letters 267(1) (1990) 99–102.
687 [30] T.L. Bailey, M. Boden, F.A. Buske, M. Frith, C.E. Grant, L. Clementi, J. Ren, W.W.
688 Li, W.S. Noble, MEME Suite: tools for motif discovery and searching, Nucleic
689 Acids Research 37(suppl_2) (2009) W202–W208.
690 [31] C. Chen, H. Chen, Y. Zhang, H.R. Thomas, M.H. Frank, Y. He, R. Xia, TBtools:
691 an integrative toolkit developed for interactive analyses of big biological data,
692 Molecular plant 13(8) (2020) 1194–1202.
693 [32] Y. Tao, A.F. van Peer, Q. Huang, Y. Shao, L. Zhang, B. Xie, Y. Jiang, J. Zhu, B.
694 Xie, Identification of novel and robust internal control genes from *Volvariella*
695 *volvacea* that are suitable for RT-qPCR in filamentous fungi, Scientific Reports
696 6(1) (2016) 29236.
697 [33] K.J. Livak, T.D. Schmittgen, Analysis of relative gene expression data using real-
698 time quantitative PCR and the $2^{-\Delta\Delta CT}$ method, methods 25(4) (2001) 402–408.
699 [34] L. Hou, L. Wang, X. Wu, W. Gao, J. Zhang, C. Huang, Expression patterns of two
700 pal genes of Pleurotus ostreatus across developmental stages and under heat stress,
701 BMC microbiology 19(1) (2019) 231.
702 [35] M. Melgosa, E. Hita, J. Romero, L.J. del Barco, Color-discrimination thresholds
703 translated from the CIE (x, y, Y) space to the CIE 1976 (L*, a*, b*), Color

Research & Application 19(1) (1994) 10–18.

[36] J.-L. Tian, A. Ren, T. Wang, J. Zhu, Y.-R. Hu, L. Shi, H.-S. Yu, M.-W. Zhao, Hydrogen sulfide, a novel small molecule signalling agent, participates in the regulation of ganoderic acids biosynthesis induced by heat stress in *Ganoderma lucidum*, Fungal Genetics and Biology 130 (2019) 19–30.

[37] K. Li, M. Wang, R. Wang, XiaojuanJiao, HongchaoZhao, JingpengZhou, YunleiLi, HaifangLin, Hai, Hydrogen Sulfide Regulates Glucose Uptake in Skeletal Muscles via S-Sulfhydration of AMPK in Muscle Fiber Type-Dependent Way, The Journal of Nutrition: Official Organ of the American Institute of Nutrition 153(10) (2023) 2878–2892.

[38] M. Lescot, P. Déhais, G. Thijs, K. Marchal, Y. Moreau, Y. Van de Peer, P. Rouzé, S. Rombauts, PlantCARE, a database of plant cis-acting regulatory elements and a portal to tools for in silico analysis of promoter sequences, Nucleic acids research 30(1) (2002) 325–327.

[39] M.N. Cheng, Z.J. Huang, Q.Z. Hua, W. Shan, J.F. Kuang, W.J. Lu, Y.H. Qin, J.Y. Chen, The WRKY transcription factor HpWRKY44 regulates CytP450-like1 expression in red pitaya fruit (*Hylocereus polyrhizus*), Hortic Res 4 (2017) 17039.

[40] H. Chen, Y. Zou, Y. Shang, H. Lin, Y. Wang, R. Cai, X. Tang, J.-M. Zhou, Firefly luciferase complementation imaging assay for protein-protein interactions in plants, Plant physiology 146(2) (2008) 368.

[41] Q. Su, F. Zhang, Y. Xiao, P. Zhang, H. Xing, F. Chen, An efficient screening system to identify protein-protein or protein-DNA interaction partners of rice transcription factors, Journal of genetics and genomics= Yi chuan xue bao 49(10) (2022) 979–981.

[42] B. Deng, W. Wang, C. Ruan, L. Deng, S. Yao, K. Zeng, Involvement of CsWRKY70 in salicylic acid-induced citrus fruit resistance against *Penicillium digitatum*, Horticulture Research 7 (2020) 157.

[43] S. Kilaru, P.J. Hoegger, U. Kües, The laccase multi-gene family in *Coprinopsis cinerea* has seventeen different members that divide into two distinct subfamilies, Curr Genet 50(1) (2006) 45–60.

[44] E. Morin, A. Kohler, A.R. Baker, M. Foulongne-Oriol, V. Lombard, L.G. Nagy, R.A. Ohm, A. Patyshakuliyeva, A. Brun, A.L. Aerts, A.M. Bailey, C. Billette, P.M. Coutinho, G. Deakin, H. Doddapaneni, D. Floudas, J. Grimwood, K. Hildén, U. Kües, K.M. Labutti, A. Lapidus, E.A. Lindquist, S.M. Lucas, C. Murat, R.W. Riley, A.A. Salamov, J. Schmutz, V. Subramanian, H.A. Wösten, J. Xu, D.C. Eastwood, G.D. Foster, A.S. Sonnenberg, D. Cullen, R.P. de Vries, T. Lundell, D.S. Hibbett, B. Henrissat, K.S. Burton, R.W. Kerrigan, M.P. Challen, I.V. Grigoriev, F. Martin, Genome sequence of the button mushroom *Agaricus bisporus* reveals mechanisms governing adaptation to a humic-rich ecological niche, Proc Natl Acad Sci U S A 109(43) (2012) 17501–6.

[45] S.V. Kumar, P.S. Phale, S. Durani, P.P. Wangikar, Combined sequence and structure analysis of the fungal laccase family, Biotechnol Bioeng 83(4) (2003) 386–94.

[46] R. Biłas, K. Szafran, K. Hnatuszko-Konka, A.K. Kononowicz, Cis-regulatory elements used to control gene expression in plants, Plant Cell, Tissue and Organ Culture (PCTOC) 127(2) (2016) 269–287.

[47] J. Zhou, F. Hu, M. Berhe, R. Zhou, D. Li, H. Li, L. Yang, T. Zhou, Y. Zhang, L. Wang, J. You, Genome-wide identification, classification, and expression profiling of *LAC* gene family in sesame, BMC Plant Biology 24(1) (2024) 1254.

[48] S.J. Sun, J.Z. Liu, K.H. Hu, H.X. Zhu, The level of secreted laccase activity in the edible fungi and their growing cycles are closely related, Curr Microbiol 62(3) (2011) 871–5.

[49] J. Zhang, H. Chen, M. Chen, A. Ren, J. Huang, H. Wang, M. Zhao, Z. Feng, Cloning and functional analysis of a laccase gene during fruiting body formation in *Hypsizygus marmoreus*, Microbiol Res 179 (2015) 54–63.

[50] W. Jin, J. Li, H. Feng, S. You, L. Zhang, J. Norvienyeku, K. Hu, S. Sun, Z. Wang, Importance of a Laccase Gene (*Lcc1*) in the Development of *Ganoderma tsugae*, International Journal of Molecular Sciences 19(2) (2018) 471.

[51] K. Nakade, H. Watanabe, Y. Sakamoto, T. Sato, Gene silencing of the *Lentinula edodes* lcc1 gene by expression of a homologous inverted repeat sequence, Microbiol Res 166(6) (2011) 484–93.

[52] Y. Sakamoto, K. Nakade, S. Sato, A. Yoshimi, K. Sasaki, N. Konno, K. Abe, Cell wall structure of secreted laccase-silenced strain in *Lentinula edodes*, Fungal Biol 122(12) (2018) 1192–1200.

[53] P.J. Vonk, R.A. Ohm, The role of homeodomain transcription factors in fungal development, Fungal Biology Reviews 32(4) (2018) 219–230.

[54] H. Guo, Y. Wang, L. Wang, P. Hu, Y. Wang, Y. Jia, C. Zhang, Y. Zhang, Y. Zhang, C. Wang, C. Yang, Expression of the MYB transcription factor gene BplMYB46 affects abiotic stress tolerance and secondary cell wall deposition in *Betula platyphylla*, Plant Biotechnol J 15(1) (2017) 107–121.

[55] R. Yang, Q. Wang, Y. Wang, X. Zhang, X. Zheng, Y. Li, D. Prusky, Y. Bi, Y. Han, MYB168 and WRKY20 transcription factors synergistically regulate lignin monomer synthesis during potato tuber wound healing, Plant Physiology 197(1) (2025) kiae573.

Supplementary Files

This is a list of supplementary files associated with this preprint. Click to download.

- SupplementaryMaterial.docx